07.2;13.1

Investigation of metal-insulator-semiconductor structure based on CdHgTe and HfO_2

© D.V. Gorshkov, E.R. Zakirov, G.Y. Sidorov, I.V. Sabinina, D.V. Marin

Rzhanov Institute of Semiconductor Physics, Siberian Branch, Russian Academy of Sciences, Novosibirsk, Russia
E-mail: GorshkovDV@isp.nsc.ru

Received June 14, 2022
Revised August 11, 2022
Accepted August 17, 2022

The interface between $Cd_{0.22}Hg_{0.78}Te$ and HfO_2 grown by plasma-enhanced atomic layer deposition at a temperature of 120°C in a specifically optimized deposition mode has been studied. The method used in this work for measuring the admittance of metal–dielectric–semiconductor structures made it possible to establish that their electrophysical parameters are uniform over the sample surface. The spectrum of fast surface states density at the $HfO_2-Cd_{0.22}Hg_{0.78}Te$ interface has been calculated.

Keywords: CdHgTe, HfO_2, ALD, C-V, passivating coating.

DOI: 10.21883/TPL.2022.10.54789.19279

Mercury cadmium telluride $Cd_xHg_{1-x}Te$ (MCT) solid solutions are used widely in the design and fabrication of lasers [1] and photodetector arrays for the middle [2] and long [3] infrared ranges and in the studies of topological insulators [4]. Surface passivation is one of the key process steps for such devices, since the interface quality has a considerable influence on their characteristics. In view of the fact that a number of these devices are subjected to thermal cycling, fine adhesion to MCT is required from a passivating coating [5]. Advances in the atomic layer deposition (ALD) technology rendered it possible to deposit various types of insulator coatings with a high degree of control over the process even at relatively low temperatures. It has been demonstrated in [6] that Al_2O_3 deposited onto MCT by ALD has somewhat better passivating properties that a CdTe/ZnS coating. The authors of [7–9] have found that Al_2O_3 deposited onto MCT by plasma-enhanced ALD (PE-ALD) at a temperature of 120°C acquires fine passivating characteristics. It has been established in several studies into passivation of narrow-gap A_3B_5 semiconductors that HfO_2 provides a higher-quality interface than Al_2O_3 [10,11]. However, the standard PE-ALD temperature window of an almost constant growth rate per cycle (GRP) for HfO_2 is at 160-340°C [10,12,13]. These values are considerably higher than the allowable temperature of MCT heating in vacuum [14]. The aim of the present study was to examine the passivating properties of a HfO_2 coating deposited onto MCT outside of the standard temperature window. The primary objective was to characterize the influence of PE-ALD process parameters on the quality of films formed at a growth temperature of 120°C.

Films of HfO_2 were grown using a FlexAL (Oxford Instruments) setup with a tetrakis(ethylmethylamino)hafnium (TEMAH) precursor that was heated to 75°C and fed into the growth chamber with a 250 sccm Ar flow (the feed time was 1 s). The same Ar flow through the growth chamber volume was supplied at the stages of pumping the remaining precursor out (the feed time was 3 s) and post-plasma pumping (PPP) the reaction products out after oxidation. At the oxidation stage, the O_2 pressure in the chamber was 15 mTorr, and the power of the inductively coupled plasma generator was 250 W (its operation time was 3 s). Just as in [13], the PPP stage duration was varied to determine the GRP saturation time. A total of 100 deposition cycles were performed for each sample at a substrate temperature of 120°C.

The ellipsometric angles after HfO_2 growth on Si were measured with a spectral ellipsometer. The thickness and the refraction index of films were then determined within the Cauchy model using the thickness value of native silicon oxide measured prior to growth. The chemical composition was analyzed by X-ray photoelectron spectroscopy using a ProvenX-ARPES (SPECS, Germany) setup fitted with a source of focused monochromatic AlK_α (1486.71 eV) radiation and an ASTRAIOS 190 hemispherical electron energy analyzer.

A heteroepitaxial $Cd_{0.22}Hg_{0.78}Te$ structure grown on a Si substrate by molecular beam epitaxy was used to examine the electrophysical properties of the HfO_2–MCT interface. Following growth, undoped MCT was annealed to obtain vacancy p-type conductivity with a hole density of $9.5 \cdot 10^{15}\,cm^{-3}$ and a hole mobility of $370\,cm^2 \cdot V^{-1} \cdot s^{-1}$. The MCT surface was not processed in any way prior to HfO_2 growth. Indium contacts 50–500 μm in diameter were deposited onto HfO_2 on MCT by thermal evaporation. The capacitance–voltage curves (CVs) of the obtained metal–insulator–semiconductor (MIS) structures were measured at a temperature of 77 K using Agilent B1500A.

It was found that the GRP assumes increasingly smaller values of 0.125, 0.119, 0.114, and 0.114 nm at a PPP duration of 2, 4, 6, and 8 s, respectively. Thus, saturation is

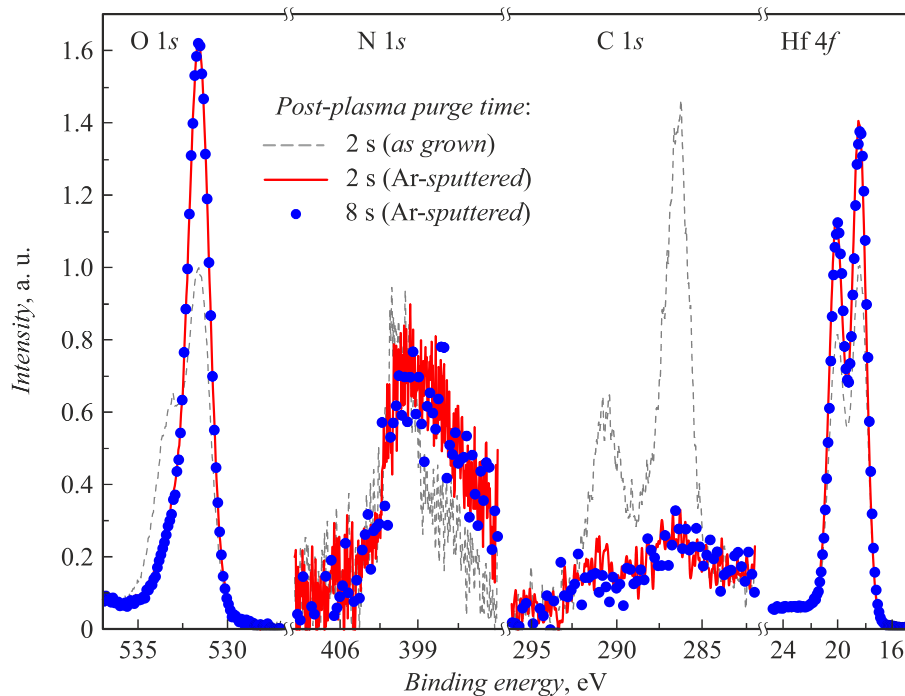

Figure 1. X-ray photoelectron O 1s, N 1s, C 1s and Hf 4f lines of HfO_2 films, which were grown by PE-ALD from a TEMAH precursor at a temperature of 120°C, for post-plasma pumping-out times of 2 s (dashed and solid curves) and 8 s (dots) before (dashed curve) and after (solid curve and dots) surface sputtering with an ion beam performed to remove the surface contamination layer.

achieved at 6 s. The GRP and the refraction index of HfO_2 films remained essentially unchanged when the chosen precursor feed time and the time of subsequent chamber purging were doubled. Thus, the following durations of PE-ALD process stages were set in the present study: 1/3/3/6 s. A HfO_2 film was also grown at a temperature of 290°C with the duration of stages set to 1/3/3/2 s. The GRP measured for it was 0.106 nm, which is close to the available literature data obtained using similar equipment: 0.104 nm [15].

The results of analysis of the chemical composition of HfO_2 films by X-ray photoelectron spectroscopy verified that hafnium atoms are in the oxidized Hf^{4+} state (the Hf $4f_{7/2}$ line has a binding energy of 18.4 eV and a FWHM of 1.2 eV); no spectrum components corresponding to hafnium suboxides or hafnium in its elemental state [16,17] were found (Fig. 1). The shape and intensity of hafnium lines in the spectrum and the ratio of integral intensities of the O 1s (with a binding energy of 532.1 eV) and Hf 4f lines were found to be independent of the PPP duration. The C 1s and N 1s lines observed in the spectra before and after etching with an ion beam are indicative of contamination of the surface and the bulk of the insulator material. It was found after cleaning of the sample surfaces that the densities of carbon and nitrogen atoms in the bulk of deposited films decrease by $\sim$ 20 and $\sim$ 5%, respectively, as the PPP duration increases from 2 to 8 s. No other contaminants were identified in HfO_2 films.

The hole density in MCT measured using the Hall probe method was $9.5 \cdot 10^{15}$ and $9.7 \cdot 10^{15}$ cm^{-3} before and after HfO_2 growth, respectively. Therefore, oxygen ions do not damage the MCT surface in this growth process.

The CVs of no less than 30 MIS structures were measured to determine the uniformity of electrophysical parameters of the HfO_2–MCT interface over the sample surface (12×24 mm in size). Figure 2 shows the CVs of structures with a contact diameter of 450 μm, which have a characteristic low-frequency form at a measurement signal frequency of 10 kHz. The voltage was swept from 0.5 to -6.0 V in order to minimize the influence of charge captured at shallow traps in the near-surface region of the semiconductor and the insulator on the shape and positioning of CVs. The inset in Fig. 2 shows that the insulator capacitance spread in the accumulation region does not exceed 1%. The spread of the flat-band voltage positioning is within 20 mV (with the voltage step and the amplitude of the variable signal being set to 10 mV). The HfO_2–MCT system exhibited a high degree of uniformity of electrophysical characteristics over the sample surface.

The spectrum of the fast surface state density (D_{it}) at the HfO_2–MCT interface was calculated in accordance with the procedure outlined in [18]. CVs were measured in the voltage range from 0.5 to -6.0 V and at frequencies ranging from 1 kHz to 1 MHz. Since charge accumulates at slow traps when a negative voltage is applied, each CV at a given frequency was measured for different MIS structures. Parallel conductance (G_p) of the equivalent circuit of the MIS structure (see the inset in Fig. 3) was then calculated

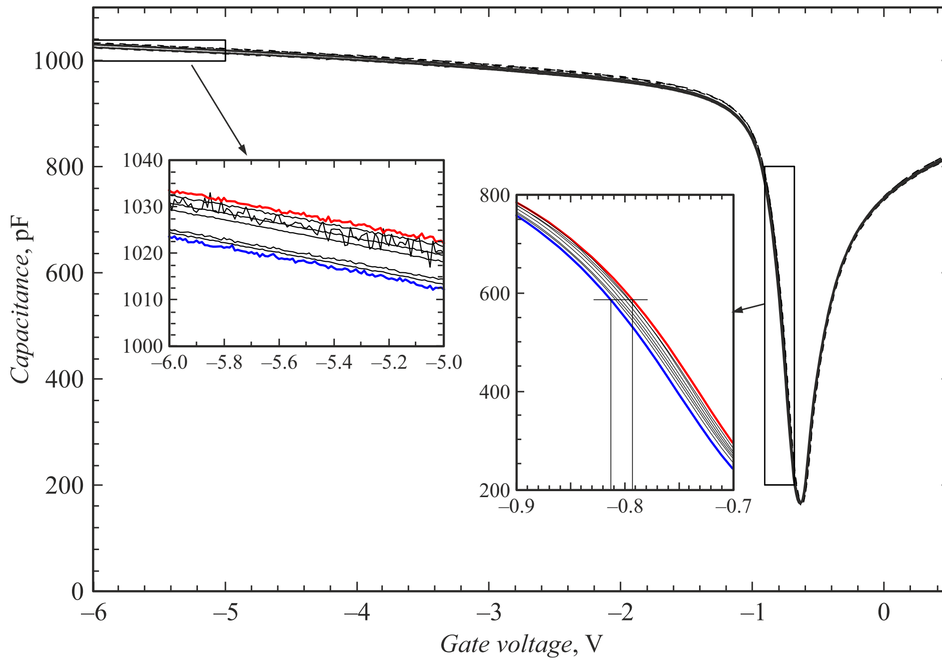

Figure 2. Capacitance–voltage curves of the fabricated $In-HfO_2-Cd_{0.22}Hg_{0.78}Te$ structures. The indium contact diameter is 450 μm. Measurements were performed at a temperature of 77 K and a measurement signal frequency of 10 kHz. The voltage was swept from 0.5 to −6.0 V. Enlarged CV fragments are shown in the insets.

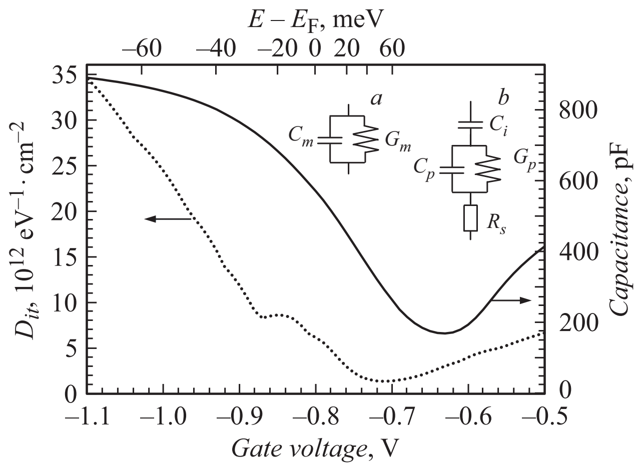

Figure 3. Surface state density distribution calculated using the conductance method (dotted curve) and CV measured at 1 kHz (solid curve). The upper axis denotes the estimated energy relative to the Fermi level (E_F). The measurement circuit and the simplified equivalent circuit of the MIS structure are shown in insets (*a*) and (*b*), respectively.

in accordance with [18] using the following formula:

$$G_p = \frac{\omega^2 C_i^2 G_m}{G_m^2 + \omega^2 (C_i - C_m)^2}, \quad (1)$$

where C_m and G_m are the measured capacitance and conductance values, C_i is the insulator film capacitance, ω is the angular frequency of a variable signal ($\omega = 2\pi f$), and C_p is the MCT capacitance (indicated in Fig. 3). The frequency dependence of G_p/ω at a constant gate voltage was plotted after that. This dependence has a well-pronounced maximum due to the recharging of surface states. Using the corresponding formula from [18], we determine D_{it}:

$$D_{it} \approx \frac{2.5(G_p/\omega)_{\max}}{Aq}, \quad (2)$$

where $(G_p/\omega)_{\max}$ is the maximum of the frequency dependence of G_p/ω at the chosen voltage, A is the contact area, and q is the electron charge. This method for D_{it} estimation yields values that are consistent with those provided by other methods [19]. Its key advantage consists in the fact that it circumvents the need to calculate the theoretical CV dependence for MCT (such calculations were performed, e,g., in [8,9]). It should be noted that formula (1) is applicable in the case when series resistance R_s is negligible. In the present experiment, the series resistance induced by the bulk resistance of *p*-type MCT started to exert a considerable influence on the CV shape at a frequency of 40 kHz, while most $(G_p/\omega)_{\max}$ values corresponded to frequencies below 30 kHz.

Figure 3 presents the dependence of density D_{it} on the metal gate voltage. The surface potential was estimated using the Berglund method. The obtained values of energy relative to the Fermi level are plotted on the upper axis with a pitch of 20 meV. The CV measured at 1 kHz is also shown in Fig. 3. Near the Fermi level, $D_{it} = 6 \cdot 10^{12}\,\text{eV}^{-1} \cdot \text{cm}^{-2}$.

No delamination or cracking of the HfO_2 film were observed after 40 cycles of sample heating and cooling. This is indicative of fine adhesion between the film and the MCT surface.

Thus, the influence of PPP duration on the GRP value and the chemical composition of HfO_2 films grown by PE-ALD from a TEMAH precursor at a temperature of 120°C was examined. It was found that the HfO_2 film capacitance and the fixed charge value are uniform over the sample surface. The D_{it} spectrum for the HfO_2−CdHgTe interface was calculated. The obtained HfO_2 feature a fine adhesion to MCT.

Funding

This work was supported by grant No. 21-72-10134 from the Russian Science Foundation.

Conflict of interest

The authors declare that they have no conflict of interest.

References

[1] V.Ya. Aleshkin, A.A. Dubinov, V.V. Rumyantsev, M.A. Fadeev, O.L. Domnina, N.N. Mikhailov, S.A. Dvoretsky, F. Teppe, V.I. Gavrilenko, S.V. Morozov, J. Phys.: Condens. Matter, **30**, 495301 (2018). DOI: 10.1088/1361-648X/aaebf5

[2] V.M. Bazovkin, V.S. Varavin, V.V. Vasil'ev, A.V. Glukhov, D.V. Gorshkov, S.A. Dvoretsky, A.P. Kovchavtsev, Yu.S. Makarov, D.V. Marin, I.V. Mzhelsky, V.G. Polovinkin, V.G. Remesnik, I.V. Sabinina, Yu.G. Sidorov, G.Yu. Sidorov, A.S. Stroganov, A.V. Tsarenko, M.V. Yakushev, A.V. Latyshev, J. Commun. Technol. Electron., **64**, 1011 (2019). DOI: 10.1134/S1064226919090043

[3] A.V. Zverev, A.O. Suslyakov, I.V. Sabinina, G.Yu. Sidorov, M.V. Yakushev, V.D. Kuzmin, V.S. Varavin, V.G. Remesnik, Yu.S. Makarov, A.V. Predein, D.V. Gorshkov, S.A. Dvoretsky, V.V. Vasil'ev, Yu.G. Sidorov, A.V. Latyshev, I.I. Kremis, J. Commun. Technol. Electron., **64**, 1024 (2019). DOI: 10.1134/S1064226919090171

[4] A.V. Galeeva, A.I. Artamkin, A.S. Kazakov, S.N. Danilov, S.A. Dvoretskiy, N.N. Mikhailov, L.I. Ryabova, D.R. Khokhlov, Beilstein J. Nanotechnol., **9**, 1035 (2018). DOI: 10.3762/bjnano.9.96

[5] Y. Nemirovsky, G. Bahir, J. Vac. Sci. Technol. A, **7**, 450 (1989). DOI: 10.1116/1.576202

[6] P. Zhang, Z.-H. Ye, C.-H. Sun, Y.-Y. Chen, T.-N. Zhang, X. Chen, C. Lin, R.-J. Ding, L. He, J. Electron. Mater., **9**, 4716 (2016). DOI: 10.1007/s11664-016-4686-z

[7] D.V. Gorshkov, G.Yu. Sidorov, I.V. Sabinina, Yu.G. Sidorov, D.V. Marin, M.V. Yakushev, Tech. Phys. Lett., **46**, 741 (2020). DOI: 10.1134/S1063785020080064.

[8] A.P. Kovchavtsev, G.Yu. Sidorov, A.E. Nastovjak, A.V. Tsarenko, I.V. Sabinina, V.V. Vasilyev, J. Appl. Phys., **121**, 125304 (2017). DOI: 10.1063/1.4978967

[9] A.V. Voitsekhovskii, S.N. Nesmelov, S.M. Dzyadukh, J. Phys. Chem. Solids, **102**, 42 (2016). DOI: 10.1016/j.jpcs.2016.10.015

[10] N. Goel, P. Majhi, C.O. Chui, W. Tsai, D. Choi, J.S. Harris, Appl. Phys. Lett., **89**, 163517 (2006). DOI: 10.1063/1.2363959

[11] N. Miyata, A. Ohtake, M. Ichikawa, T. Mori, T. Yasuda, Appl. Phys. Lett., **104**, 232104 (2014). DOI: 10.1063/1.4882643

[12] A. Hardtdegen, H. Zhang, S. Hoffmann-Eifert, ECS Trans., **75**, 177 (2016). DOI: 10.1149/07506.0177ecst

[13] A. Sharma, V. Longo, M.A. Verheijen, A.A. Bol, W.M.M.E. Kessels, J. Vac. Sci. Technol. A, **35**, 01B130 (2017). DOI: 10.1116/1.4972210

[14] E.R. Zakirov, V.G. Kesler, G.Yu. Sidorov, I.P. Prosvirin, A.K. Gutakovsky, V.I. Vdovin, Semicond. Sci. Technol., **34**, 065007 (2019). DOI: 10.1088/1361-6641/ab1961

[15] S.B.S. Heil, J.L. van Hemmen, J. Vac. Sci. Technol. A, **25**, 1357 (2007). DOI: 10.1116/1.2753846

[16] T.P. Smirnova, L.V. Yakovkina, V.N. Kitchai, V.V. Kaichev, Yu.V. Shubin, N.B. Morozova, K.V. Zherikova, J. Phys. Chem. Solids, **69**, 685 (2008). DOI: 10.1016/j.jpcs.2007.07.123

[17] D. Barreca, A. Milanov, R. Fischer, A. Devi, E. Tondello, Surf. Sci. Spectra, **14**, 34 (2007). DOI: 10.1116/11.20080401

[18] E.H. Nicollian, J.R. Brews, *MOS (metal oxide semiconductor) physics and technology* (John Wiley and Sons, Inc, 2002).

[19] R. Engel-Herbert, Y. Hwang, S. Stemmer, J. Appl. Phys., **108**, 124101 (2010). DOI: 10.1063/1.3520431